PHYSICAL REVIEW C **73**, 021301(R) (2006)

Decay-out properties of a linked superdeformed band in ^{84}Zr

C. J. Chiara,[1] D. G. Sarantites,[1] M. Montero,[1] J. O'Brien,[1] W. Reviol,[1] O. L. Pechenaya,[2] R. M. Clark,[3] P. Fallon,[3] A. Görgen,[3,*] A. O. Macchiavelli,[3] D. Ward,[3] Y. R. Shimizu,[4] and W. Satuła[5]

[1]*Chemistry Department, Washington University, St. Louis, Missouri 63130, USA*

[2]*Physics Department, Washington University, St. Louis, Missouri 63130, USA*

[3]*Nuclear Science Division, Lawrence Berkeley National Laboratory, Berkeley, California 94720, USA*

[4]*Department of Physics, Kyushu University, Fukuoka 812-8581, Japan*

[5]*Institute of Theoretical Physics, Warsaw University, Hoża 69, PL-00681 Warsaw, Poland*

(Received 18 September 2005; published 28 February 2006)

Three discrete transitions were observed between the yrast superdeformed (SD) band and states of normal deformation (ND) in the nucleus ^{84}Zr. This is the first observation of such linking transitions in the mass-80 SD region. The properties of the decay out of the SD well in ^{84}Zr are compared with those in other SD mass regions. Calculations suggest that there is extensive mixing of configurations in the SD and ND potential minima, leading to an abrupt and highly fragmented decay-out process. A study of least-action tunneling paths indicates that the potential barrier separating the SD and ND wells is very small.

DOI: 10.1103/PhysRevC.73.021301 PACS number(s): 23.20.Lv, 21.10.Re, 27.50.+e

Superdeformed (SD) bands, where the atomic nucleus exhibits a large (nearly 2:1) axis ratio, have been observed in several distinct mass regions across the nuclear chart [1]. In a limited number of these cases, discrete transitions connecting states in the SD and normal-deformed (ND) potential wells have been observed. The observation of such "linking" transitions is of vital importance in studying the SD phenomenon—not only does it provide excitation energies and possibly the spins and parity of the band, but the decay mechanism itself responsible for the rapid depopulation of the SD well may also be explored.

The nature of the observed decay out can be quite different for the various mass regions. For example, in the mass $A \approx 40$ region, the decay tends to proceed via intense $E2$ transitions, due to strong mixing of a small number of configurations [2–4]. In contrast, the observed links in the $A \approx 150$ [5] and 190 [6] regions carry only a small fraction of the SD intensity, and generally include weak, statistical $E1$ decays. In the $A \approx 60$ and 130 regions, the nuclei are not as deformed as in the other regions [1], and it has been found that the first and second potential minima are not well separated by any significant barrier (e.g., Refs. [7,8]). Here, a sizable fraction of the decay-out intensity is observed. The $A \approx 130$ and some $A \approx 60$ SD nuclei tend to decay out (much) nearer the yrast line than found in other regions [1]. Other $A \approx 60$ nuclei are unique in that they prompt-particle decay out of the SD well (e.g., Refs. [8,9]). Clearly there is a variety of decay modes, making it difficult to formulate a cohesive picture that applies to SD bands in general.

The $A \approx 80$ SD nuclei comprise the one major SD region that had not been previously linked. In the current study, the "central" $A \approx 80$ SD nucleus [10], ^{84}Zr, has been linked. In this Rapid Communication, we show the properties of the ^{84}Zr decay out, and how it compares with other SD regions. With the first linked band in an $A \approx 80$ SD nucleus, ^{84}Zr provides access to information on the decay properties in an entirely new mass region.

High-spin states in ^{84}Zr were populated via the ^{58}Ni(^{32}S,$\alpha 2p$) reaction. A 140-MeV ^{32}S beam, provided by the 88-Inch Cyclotron at Lawrence Berkeley National Laboratory, was directed onto a self-supporting 0.50-mg/cm^2 ^{58}Ni target. The Gammasphere [11] and Microball [12] arrays were used to detect γ rays and charged particles, respectively. Gammasphere consisted of 102 Compton-suppressed HPGe detectors arranged in 16 rings of constant angle θ relative to the beam. A total of 2.2×10^9 events with γ-ray fold five or higher were recorded, along with any correlated Microball pulse-height and timing information. The efficiencies for detecting protons and α particles were $\varepsilon_p \approx 80\%$ and $\varepsilon_\alpha \approx 70\%$, respectively. Events were selected offline which included exactly one α particle and one or two protons. A total of 402×10^6 such events were unfolded into constituent threefold γ coincidences and their energies E_γ incremented into an $E_\gamma - E_\gamma - E_\gamma$ histogram (cube). The RADWARE analysis package [13] was used to project background-subtracted $\gamma\gamma$-gated spectra from the cube.

A partial level scheme of ^{84}Zr, deduced from the coincidence cube, is presented in Fig. 1; only those ND bands relevant to the decay from the SD well are shown (for spins $I \geqslant 14$). These results confirm the decay schemes of Refs. [14,15]. An excited SD band was observed in addition to the yrast SD1 band; this will be discussed separately [16].

Double gates were placed on pairs of γ rays in band SD1. The high-energy part of the spectrum resulting from the sum of all possible double gates within the band is shown in Fig. 2(a). The three transitions marked with asterisks in this spectrum, at 3464, 3743, and 4052 keV, are candidates for the decay out of the band. Double gating on one of these transitions and the members of band SD1 yields the spectra presented in Figs. 2(b)–(d). In each of these spectra, members of band SD1 are clearly present. In addition, each of the transitions is in coincidence with a different ND structure: 4052 and 3464 keV

*Present address: DAPNIA/SPhN, CEA Saclay, F-91191 Gif-sur-Yvette Cedex, France.

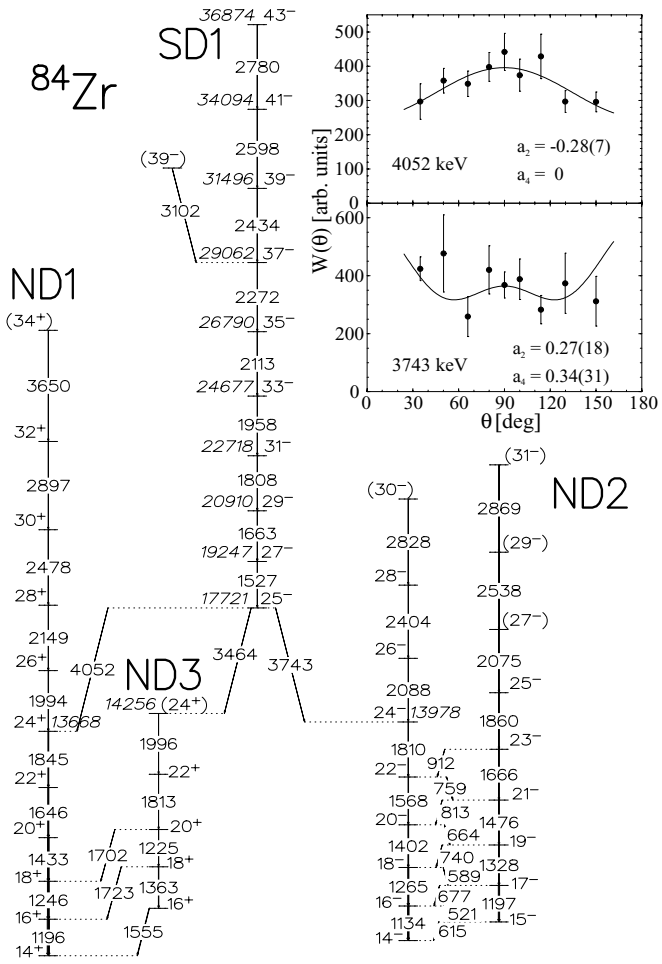

FIG. 1. Partial level scheme of ^{84}Zr. Energies of states (in italics) and transitions are in keV. Tentative spin assignments are given in parentheses. Inset: ADs for two of the links. The a_4 coefficient for the 4052-keV transition was found to be consistent with zero; it was subsequently fixed as zero and a_2 was refitted, yielding the same results (within errors).

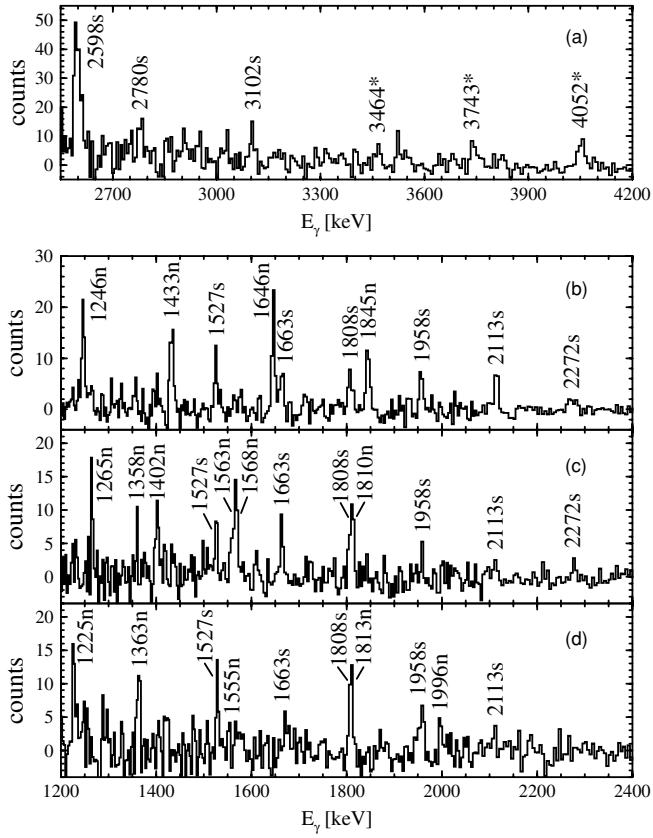

FIG. 2. Background-subtracted γ-ray energy spectra created from double gates on the following transitions, where S is the set of all γ rays in band SD1: (a) S/S (excluding self-coincidences), (b) S/4052, (c) S/3743, and (d) S/3464. Peaks are labelled with their energies in keV and an 's' or 'n' for SD or ND transitions, respectively; those marked with an asterisk in (a) are identified linking transitions. The peaks at 1358 and 1563 keV in (c) arise from the decays from ND2 to ND1 at low spins (not shown in Fig. 1).

with positive-parity bands ND1 and ND3, respectively, and 3743 keV with negative-parity band ND2. Energy sums and coincidence relationships allow an unambiguous placement of the 4052-, 3743-, and 3464-keV γ rays decaying out of the lowest state of band SD1 into the 24^+, 24^-, and (24^+) states of bands ND1, ND2, and ND3, respectively. Thus, these single-step linking transitions between the SD and ND wells of ^{84}Zr fix the excitation energies of the states in band SD1. Several of the unlabelled peaks in Fig. 2(a) are, like the three listed above, statistically ($>2\sigma$) above background, but only the latter could be confirmed as discrete transitions from band SD1 to ND states. For example, double-gating on the SD1 transitions and the composite peak at around 3540 keV does not yield an unambiguous ND spectrum such as those shown in Figs. 2(b)–(d). Some of these may be involved in multistep decay paths that could not be resolved in this work.

The intensity of band SD1 ($I_{\rm SD1}$) is about 3% that of the $2^+ \rightarrow 0^+$ 540-keV ground-state transition (not shown). Of this, only about 2% of the $I_{\rm SD1}$ intensity passes through the observed linking transitions, with the 4052-, 3743-, and 3464-keV transitions carrying about 0.9%, 0.7%, and 0.4% of $I_{\rm SD1}$, respectively. The remaining 98% of the SD1 decay has not been identified in this analysis. Fractions of this intensity are likely carried by additional high-energy transitions that could not be placed in the level scheme, such as the unlabelled peaks in Fig. 2(a), or by even weaker (quasicontinuum) transitions that are not resolved from background. Although rapid depopulation is a common feature among SD bands in all mass regions, the decay out in ^{84}Zr seems to occur even more abruptly over only two levels. The 1527-keV transition carries 65% of the intensity of the 1663-keV transition (the maximum for the band), with no additional in-band transitions observed below it.

Gated angular distributions (ADs) were measured to determine the multipolarities of the linking transitions: the γ-ray intensities were measured at several angles in spectra gated on the lowest five members of band SD1, and fitted with the function $W(\theta) = a_0[1 + a_2 P_2(\cos\theta) + a_4 P_4(\cos\theta)]$. The fits for the 4052- and 3743-keV transitions are shown in the

inset of Fig. 1 (the third link is too weak to fit). The AD of the 4052-keV transition is consistent with a pure stretched dipole assignment, whereas the 3743-keV transition appears to have mixed multipolarity. These two links feed bands of opposite parities, and since an $E1/M2$ admixture for the 3743-keV link is unlikely, the most consistent assignment is with $\Delta I = 1$ $E1$ and $M1/E2$ multipolarities for the 4052- and 3743-keV transitions, respectively. The lowest observed state in band SD1 is thus assigned $I^\pi = 25^-$, which is $4\hbar$ larger than estimated in Ref. [14]. These results are consistent with the previous assignment of the $\nu 5^2 \pi 5^1$ configuration to this band, i.e., two neutrons and one proton in $h_{11/2}$ intruder orbitals [10]. Furthermore, the excitation energies and aligned angular momenta of the SD band are reasonably well reproduced by cranked Strutinsky calculations similar to those presented in Ref. [10] (details will be given in Ref. [16]). This configuration is found to have $\varepsilon_2 \approx 0.50$ and γ near 0°. In Ref. [15], bands ND1, ND2, and ND3 were assigned unpaired configurations involving excitations from the *fp* shell into $g_{9/2}$ orbitals, but not into $h_{11/2}$ intruders; the calculated deformations at $I \approx 24$ are $\varepsilon_2 \approx 0.18$, $\gamma \approx -40^\circ$ for ND1 [15], $\varepsilon_2 \approx 0.18$, $\gamma \approx -50^\circ$ for ND2 [15], and a noncollective $\varepsilon_2 \approx 0.04$, $\gamma \approx +60^\circ$ for ND3 [17]. Clearly, the configurations and shapes of these ND structures are quite different from that of the SD band.

The lifetime of the 25^- state in SD1 was deduced to be $\tau = 20^{+58}_{-14}$ fs from the fractional Doppler shifts observed in this experiment. The details of this analysis will be presented in a forthcoming article [16]. Although these uncertainties are large, the measurement is sufficient to give the order of magnitude for the $B(E1)$ strengths, namely 10^{-6} W.u. for the 4052- and 3464-keV $E1$ links. Similarly, the $M1$ strength of the mixed-$M1/E2$ 3743-keV transition is estimated as $B(M1) \lesssim 10^{-4}$ W.u. Only an upper limit on $B(M1)$ is possible because the amount of $E2$ admixture cannot be reliably determined from these data.

The properties of band SD1 in ^{84}Zr can now be compared with those of SD nuclei in other regions in which discrete, single-step links have been observed. The yrast SD band in ^{152}Dy [5], the sole such example for the $A \approx 150$ region, and band SD1 in ^{84}Zr share several common features: decay out at similar excitation above yrast ($\sim$3 MeV), through very weak [$\sim$1% intensity, $B(E1) \sim 10^{-6}$ W.u.] $E1$ transitions, and from states at around $I = 25$. Weak $E1$ links are also characteristic of the $A \approx 190$ SD region. This is in contrast with the intense decays observed around $A \approx 40$ and in some cases around $A \approx 60$, where a few strong $E2$ transitions connect the SD and ND states, and the decay occurs at fairly low spins and excitation energies above yrast [2,4]. Statistical-decay models have been applied in the interpretations of the weak SD decay out in ^{152}Dy and several $A \approx 190$ nuclei (see Ref. [18] and references therein); the similarities between ^{84}Zr and those heavier SD nuclei suggest that a related approach can be used here. The decays observed between the SD and ND bands, which are associated with very different configurations and shapes, could in this way be explained as arising from small admixtures of several different configurations.

We follow the fully statistical formalism of Ref. [19] (GW model) to obtain, for a given spin, a spreading width $\Gamma^\downarrow$, which is a measure of the mixing of states in the SD and ND wells. The input parameters for the GW model are the SD (Γ_S) and ND (Γ_N) decay widths, the ND level spacing d, and the fraction F_S of intensity remaining within the SD band. The parameters used in this calculation are given in Table I. The SD widths were taken from the lifetimes of the 27^- and 25^- SD1 states, respectively, which were in turn deduced from the measured quadrupole moment ($Q_t = 5.0\,e$ b) for this band [16]. (Note that the deduced Q_t is an average value for the band; it is possible that the value near the decay-out spin may be lower due to admixtures of the SD and other configurations, as was found in ^{40}Ca [3], but the amount has not been quantified.) The ND decay widths include an $E2$ contribution, estimated similarly to Γ_S using $Q_t = 2.0\,e$ b [15] for the ND states, plus a $\sim$1-meV statistical $E1$ contribution as given in Eq. (17) of Ref. [20]. The level spacing $d = 1/\rho_{\rm FG}$, where $\rho_{\rm FG}$ is the Fermi-gas density of states [also taken from Ref. [20], Eq. (14)]; $\rho_{\rm FG}$ was calculated at energies U above yrast with level density parameter $a = 9.9\,{\rm MeV}^{-1}$. A zero backshift was assumed for these high-spin states in ^{84}Zr; i.e., a correction to U for a static pairing gap was deemed unnecessary. The intensity fraction $F_S(25)$ is an estimated upper limit since there are no in-band SD decays observed parallel to the links.

TABLE I. Parameters for the GW-model calculations.

I^π	Γ_S (meV)	Γ_N (meV)	d (keV)	U (MeV)	F_S	$\Gamma^\downarrow$ (keV)
25^-	35	28	3.5	3.0	<0.2	>3.7
27^-	60	39	7.1	2.5	0.65	0.27

Using the above parameters with the approximation given by Eq. (29) in Ref. [19], we estimate $\Gamma^\downarrow(27) = 0.27$ keV and $\Gamma^\downarrow(25) > 3.7$ keV for the 27^- and 25^- SD states in ^{84}Zr, respectively. The lower limit for $\Gamma^\downarrow(25)$ comes from the upper limit on $F_S(25)$. These values of $\Gamma^\downarrow$ are several orders of magnitude larger than in ^{152}Dy or in the $A \approx 190$ region; of the cases considered, only ^{192}Pb is comparable, with $\Gamma^\downarrow \sim 1$ keV scale (see Table II of Ref. [18]). In fact, the four quantities Γ_S, Γ_N, d, and $\Gamma^\downarrow$ in ^{84}Zr all extend the previously observed ranges to larger values, exploring a different regime from that accessed by the $A \approx 150$ and 190 studies. The ND level spacing for ^{84}Zr is up to two orders of magnitude larger than in the $A \approx 150$ and 190 cases considered [18], and thus there are fewer ND states available with which the SD states can mix; however, the ND states in ^{84}Zr also have much larger decay widths. The ratio Γ_N/d, which is relevant in the GW model, is about 1–2 orders of magnitude larger in ^{84}Zr than in ^{192}Pb, yet the spreading widths are comparable. This emphasizes the fact that both the SD and ND properties are important in determining the spreading width.

One might speculate that for low level densities like in ^{84}Zr, a two-level mixing model such as that proposed in Ref. [21] (CSB model) would be more appropriate than the above GW model that uses an ensemble of ND states. We find that the CSB approach yields a negative value for $\Gamma^\downarrow(25^-)$. The authors of Ref. [21] suggest that this may be an indication that the decay-out intensity is overestimated. This explanation is unsatisfying in the present case: it requires the intensity remaining within the SD band at this state to be several times more than what

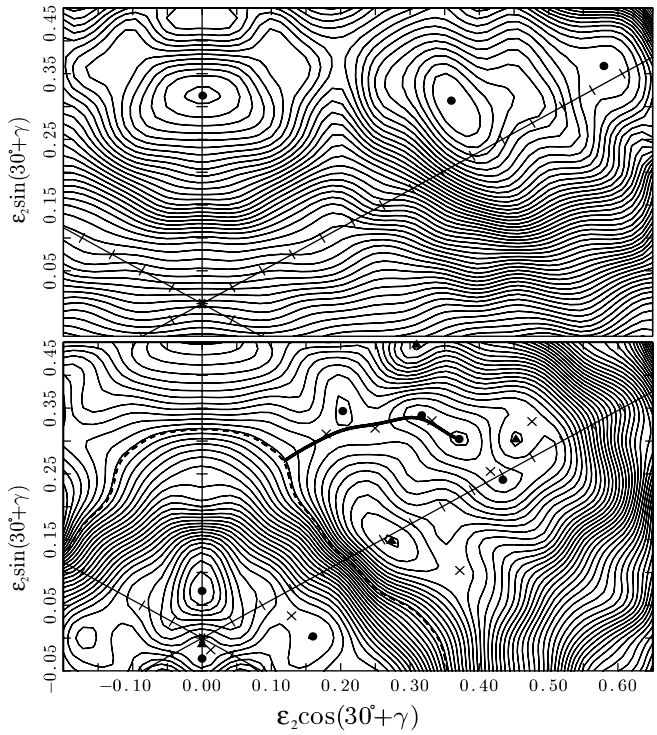

FIG. 3. Potential-energy surfaces for ^{84}Zr at spins $43\hbar$ (top) and $25\hbar$ (bottom). Circles, X's, and triangles mark local minima, saddle points, and maxima, respectively. The upsloping axis is the line for $\gamma = 0^\circ$ (collective prolate). The energy scale is 200 keV/contour. In the lower panel, the thick solid line is the least-action tunneling path, and the dashed line is the contour for the ND well at the energy of the SD minimum.

is observed. Likewise, Γ_N may have been underestimated, but to obtain $\Gamma^{\downarrow}(25^-) > 0$ would again require ND collectivity several times larger than observed (near yrast). Alternatively, more than one ND state may be involved in the mixing [21], which tends to support the usage of the GW model.

A large value for $\Gamma^{\downarrow}$ suggests that there is extensive mixing between the SD and ND minima in ^{84}Zr, and may be an indication of a small potential barrier separating the two wells. To explore the behavior of the potential barrier, we have performed calculations following the method described in Refs. [20,22]. These calculations employ a Nilsson potential and include both static and dynamic pairing correlations by using the random phase approximation [23]. Potential-energy surfaces (PES's) were generated as a function of odd (interpolated) spins and negative parity, as is appropriate for band SD1. Figure 3 shows examples of the potential surfaces for $I = 43$ (top) and 25 (bottom), the limits of observed states in the band. At each spin for which the SD minimum was calculated as nonyrast ($I \leqslant 33$), the least-action tunneling path from the SD well to the ND well, and the barrier height along that path, were determined. An example of a tunneling path (thick solid line) is shown in the $I = 25$ surface connecting the SD minimum with the equipotential ND contour. At high spins the SD minimum is well defined and yrast. With decreasing spin, however, it quickly spreads in deformation

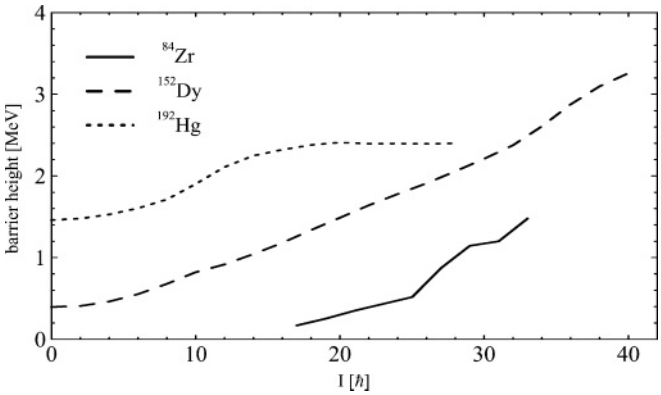

FIG. 4. Barrier height along the least-action tunneling path as a function of spin, calculated for the yrast SD bands in representative nuclei in the $A \approx 80$, 150, and 190 regions. ZPEs have not been subtracted from the barrier heights. The SD minimum for ^{84}Zr could not be followed below $I = 17\hbar$.

space and overlaps ND shapes as well as other (near-)SD shapes, becoming a broad, shallow minimum, as seen in the lower panel of Fig. 3. (A topography similar to the lower panel is also obtained through constrained self-consistent Hartree-Fock calculations [24].) The barrier separating the SD and ND wells at lower spins is very small. In this regard, ^{84}Zr is like SD nuclei in the $A \approx 60$ and 130 regions which do not have distinct barriers.

In principle, one could obtain a tunneling width based on the action S calculated from these tunneling paths (Eq. 3.1 in Ref. [22]), for comparison with $\Gamma^{\downarrow}$ of the GW model. This generally works if S is large, but the semiclassical treatment used here is invalid for small ($S \lesssim 1\hbar$) values. In ^{84}Zr, the potential between the SD and ND wells is sufficiently shallow that S does not become large enough to obtain a legitimate tunneling width near the decay-out spin; in fact, the barrier height is even smaller than the estimated zero-point energy (ZPE), and then $S = 0$. Using a different parametrization of the nuclear potential may reveal the presence of a more discernible barrier; the tunneling width and, subsequently, the SD intensity profile could then be calculated and compared with the observed data [25]. Such tunneling studies could probe details of the potential surface *between* the SD and ND minima, providing information not generally accessible in high-spin studies. It should also be noted that these calculations, using a Nilsson potential, overestimate by more than 1 MeV the energy of the SD band with respect to the yrast line at the decay-out spin; Woods-Saxon calculations provide better agreement [16]. Thus, it would be worthwhile to compare the least-action paths using a Woods-Saxon potential with those presented here [26].

Figure 4 compares the calculated potential barrier height relative to the SD minimum (i.e., no ZPE subtracted) along the tunneling path as a function of spin in ^{84}Zr, ^{152}Dy, and ^{192}Hg. It is evident that the barrier heights are considerably smaller in ^{84}Zr than in the other nuclei. In fact, over the entire range of spins ($I \leqslant 33$) in which the ^{84}Zr SD band is calculated to be nonyrast, and tunneling to the ND well could occur, the barrier height is *always* smaller than that of ^{152}Dy at $I = 28$,

its observed decay-out spin [5]. Despite this, in the data the ^{84}Zr SD intensity is found to remain "trapped" within the band until spin $27\hbar$ and below before decay out is observed. Thus, the height of the barrier is not the primary factor regulating the decay out in this nucleus.

For comparison, PES's for ^{84}Zr were also calculated using the same parametrization of the nuclear potential but without pairing, and compared to representative cases from the $A \approx 60$, 150, and 190 regions (with and without pairing). Although static pairing does not play a major role within the potential minima near the decay-out spin in ^{84}Zr, the barrier region can still be considerably influenced by the presence of pairing, thus altering the rather complicated topography of the PES. In contrast, pairing is important within the potential minima in the $A \approx 190$ SD nuclei, but it does not significantly alter the overall simpler topography. Generally speaking, the complexity of the ^{84}Zr topography appears to make this case more sensitive to factors that affect the PES, such as pairing and the choice of parametrization of the potential, than other considered examples from the $A \approx 60$, 150, and 190 regions. This makes ^{84}Zr a theoretical challenge to study. Both the PES and the mass parameters, for which pairing correlations play an important role [27], are crucial factors in evaluating the tunneling probability. Consequently, more careful treatment of the dynamics of the collective motion in the quadrupole degrees of freedom is necessary to better understand the observed behavior, especially in situations such as in ^{84}Zr where the PES is shallow. A more elaborate theoretical framework such as using the generator coordinate method [28] and consideration of the diabaticity of the large amplitude collective motion [29] may be required to study such cases.

To summarize, the yrast SD band in ^{84}Zr has been connected to states in the ND well by discrete, single-step transitions, allowing the determination of the spins, parity, and excitation energies of the SD states. The linking transitions were found to be rather weak dipole transitions, much like those observed in the $A \approx 150$ and 190 regions. The properties of the SD decay out in ^{84}Zr are similar to ^{152}Dy in several respects—excitation above yrast, decay-out spin, $B(E1)$ strengths—yet the mixing between the SD and ND wells appears to be much larger in ^{84}Zr than in ^{152}Dy, and there is a smaller barrier separating the two potential minima in ^{84}Zr, more closely resembling the $A \approx 60$ and 130 regions.

This work was supported in part by the U.S. Department of Energy under Grant No. DE-FG02-88ER-40406 and Contract No. DE-AC03-76SF-00098, and the Polish Committee for Scientific Research, Contract No. 1 P03B 059 27.

[1] B. Singh, R. Zywina, and R. B. Firestone, Nucl. Data Sheets **97**, 241 (2002).
[2] E. Ideguchi *et al*., Phys. Rev. Lett. **87**, 222501 (2001).
[3] C. J. Chiara *et al*., Phys. Rev. C **67**, 041303(R) (2003).
[4] C. E. Svensson *et al*., Phys. Rev. Lett. **85**, 2693 (2000).
[5] T. Lauritsen *et al*., Phys. Rev. Lett. **88**, 042501 (2002).
[6] For example: T. L. Khoo *et al*., Phys. Rev. Lett. **76**, 1583 (1996); A. N. Wilson *et al*., *ibid*. **90**, 142501 (2003); R. Krücken *et al*., Phys. Rev. C **55**, R1625 (1997).
[7] C. E. Svensson *et al*., Phys. Rev. Lett. **79**, 1233 (1997); A. V. Afanasjev and I. Ragnarsson, Nucl. Phys. **A608**, 176 (1996).
[8] C. Andreoiu *et al*., Phys. Rev. Lett. **91**, 232502 (2003).
[9] D. Rudolph *et al*., Phys. Rev. Lett. **86**, 1450 (2001).
[10] F. Lerma *et al*., Phys. Rev. C **67**, 044310 (2003).
[11] I. Y. Lee, Nucl. Phys. **A520**, 641c (1990).
[12] D. G. Sarantites *et al*., Nucl. Instrum. Methods Phys. Res. A **381**, 418 (1996).
[13] D. C. Radford, Nucl. Instrum. Methods Phys. Res. A **361**, 297 (1995).
[14] H.-Q. Jin *et al*., Phys. Rev. Lett. **75**, 1471 (1995).
[15] R. Cardona *et al*., Phys. Rev. C **68**, 024303 (2003).
[16] C. J. Chiara *et al*. (to be published).
[17] I. Ragnarsson, private communication.
[18] A. N. Wilson, A. J. Sargeant, P. M. Davidson, and M. S. Hussein, Phys. Rev. C **71**, 034319 (2005).
[19] Jian-zhong Gu and H. A. Weidenmüller, Nucl. Phys. **A660**, 197 (1999).
[20] K. Yoshida, M. Matsuo, and Y. R. Shimizu, Nucl. Phys. **A696**, 85 (2001).
[21] D. M. Cardamone, C. A. Stafford, and B. R. Barrett, Phys. Rev. Lett. **91**, 102502 (2003).
[22] Y. R. Shimizu, E. Vigezzi, T. Døssing, and R. A. Broglia, Nucl. Phys. **A557**, 99c (1993).
[23] Y. R. Shimizu *et al*., Rev. Mod. Phys. **61**, 131 (1989).
[24] J. Dobaczewski and J. Dudek, Comput. Phys. Commun. **131**, 164 (2000); J. Dobaczewski, J. Dudek, and P. Olbratowski, HFODD User's Guide, nucl-th/0501008.
[25] Y. R. Shimizu, M. Matsuo, and K. Yoshida, Nucl. Phys. **A682**, 464c (2001).
[26] Spin-interpolated Woods-Saxon calculations with both static and dynamic pairing correlations are in progress.
[27] Y. R. Shimizu *et al*., Phys. Lett. **B274**, 253 (1992).
[28] P.-H. Heenen, P. Bonche, J. Dobaczewski, and H. Flocard, Nucl. Phys. **A561**, 367 (1993).
[29] W. Nazarewicz, Nucl. Phys. **A557**, 489c (1993).